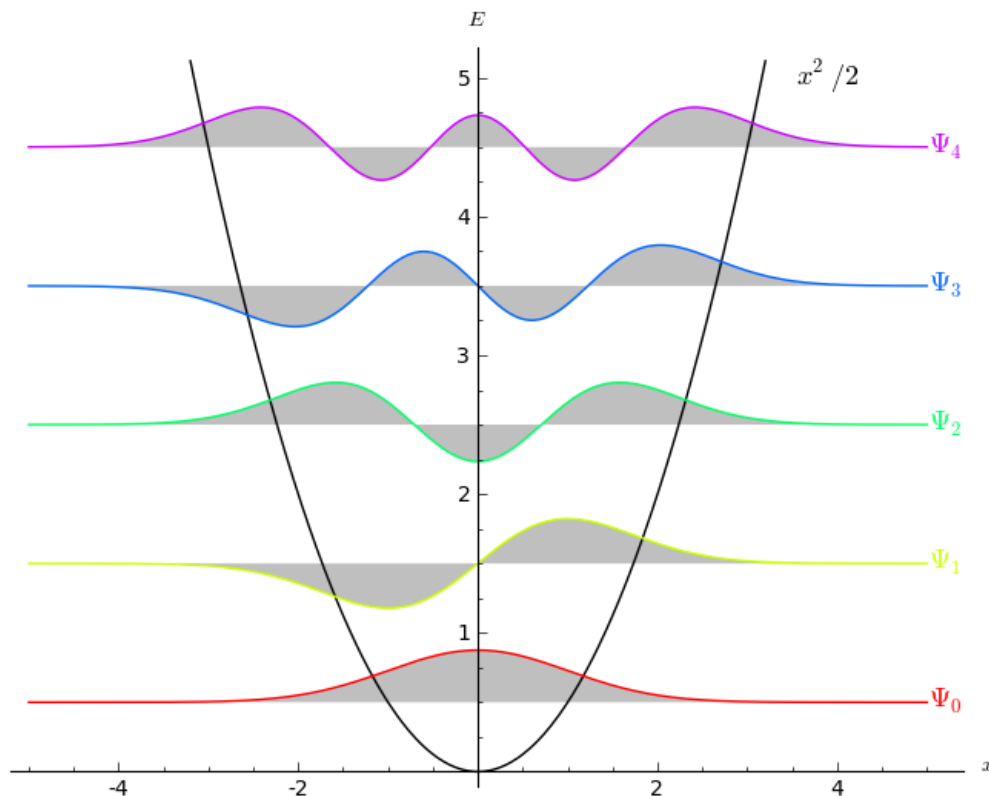


Harmonic and Anharmonic Oscillator with Path Integrals

Monte Carlo on the Lattice

Nikolas Schlage and Karthik Krishnappa Chandrashekara



Course Project submitted for Computational Physics - physics760 module

Dated: March 16, 2017

Contents

1. Theory	3
1.1. Path integral formulation in quantum mechanics	3
1.1.1. The propagator	3
1.1.2. Path integral formulation	4
1.2. Numerical evaluation of path integrals	6
1.2.1. Euclidean path integral and Euclidean action	6
1.2.2. Importance sampling in Monte Carlo Methods	7
1.2.3. Markov chains	8
1.2.4. Monte Carlo simulation of paths	10
1.3. Harmonic and anharmonic oscillator	11
1.3.1. Implementation of oscillator physics	11
1.3.2. Computation of position averages	12
1.3.3. Groundstate energy	12
2. Implementation	15
2.1. The Harmonic Oscillator	15
2.1.1. Mean Square Position	15
2.1.2. Energy Levels	16
2.1.3. Ground State Probability Density	16
2.1.4. Autocorrelation of Monte Carlo estimates of observables	17
2.1.5. Optimizing Δ	18
2.2. The Anharmonic Oscillator	19
2.2.1. Mean Square Position, Ground State Probability Density and Autocorrelation	19
3. Conclusion	21
Acknowledgement	22
Appendix	24
A. Bootstrap error analysis	25

1. Theory

1.1. Path integral formulation in quantum mechanics

1.1.1. The propagator

In the Heisenberg picture the propagator reads

$$K(x_i, t_i; x_f, t_f) = \langle x_f, t_f | x_i, t_i \rangle . \quad (1.1)$$

This quantity is called propagator due to its property of containing information about how a wave function propagates in time:

$$\psi(x_f, t_f) = \langle x_f, t_f | \psi \rangle = \int dx_i \langle x_f, t_f | x_i, t_i \rangle \langle x_i, t_i | \psi \rangle = \int dx_i K(x_i, t_i; x_f, t_f) \psi(x_i, t_i) \quad (1.2)$$

For the following calculations one has to treat time-independent kets $|x\rangle$ and operators \hat{x} so that a change to the Schrödinger picture is necessary. In the bra-ket notation, *Schrödinger's equation* becomes

$$i\hbar \frac{d}{dt} |\psi\rangle = \hat{H} |\psi\rangle \quad (1.3)$$

at which in one spatial dimension ($\hat{x} = x$) the Hamiltonian operator \hat{H} can be written as

$$\hat{H} = \frac{\hat{p}^2}{2m} + V(\hat{x}) . \quad (1.4)$$

Assuming that the initial state is a free-particle spatial state $|x_i\rangle$, the formal solution of equation (1.3) reads

$$|\psi(t)\rangle = e^{-\frac{i}{\hbar} \hat{H} t} |x_i\rangle . \quad (1.5)$$

From equation (1.5) easily follows the transition probability amplitude for a transition from the initial state $|x_i\rangle$ into a final state $|x_f\rangle$ ¹ after elapsed time $\Delta t = t_f - t_i$, namely

$$K(x_i, t_i; x_f, t_f) = \langle x_f | e^{-\frac{i}{\hbar} \hat{H} (t_f - t_i)} | x_i \rangle = \langle x_f | e^{-\frac{i}{\hbar} \hat{H} \Delta t} | x_i \rangle \quad (1.6)$$

where

$$U(t_i, t_f) := \exp\left(-\frac{i}{\hbar} \hat{H} (t_f - t_i)\right) \quad (1.7)$$

is the time evaluation operator.

¹As well as the initial state $|x_i\rangle$ the final state $|x_f\rangle$ is assumed to be a free-particle spatial state

1.1.2. Path integral formulation

According to the path integral formulation the transition amplitude can simply be written as the integral of $\exp\left(\frac{iS}{\hbar}\right)$ over all possible paths which direct from the initial to the final state² (see equation (1.18)). In order to do this the interval $[0, t]$ is divided into N infinitesimal time-step intervals so that the propagator reads

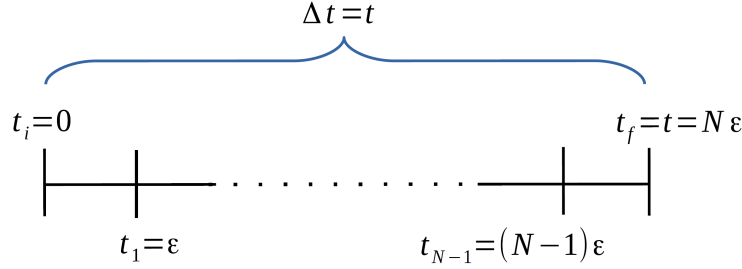


Figure 1.1.: Division of the interval $[0, t]$ into N equidistant points with distance ϵ

$$U(0, t) := e^{-\frac{i}{\hbar}\hat{H}t} = \left(e^{-\frac{i}{\hbar}\hat{H}\frac{t}{N}}\right)^N = \left(e^{-\frac{i}{\hbar}\hat{H}\epsilon}\right)^N \quad (1.8)$$

where the definition $\epsilon := \frac{\Delta t}{N} = \frac{t}{N}$ was used (Here, the initial time t_i was set to zero and the final time t_f to t). By means of equation (1.8) and the *completeness relation* $\int dx_j |x_j\rangle \langle x_j| = 1$ the transition probability can be expanded in the following way:

$$\begin{aligned} K(x_i, 0; x_f, t) &= \langle x_f | e^{-\frac{i}{\hbar}\hat{H}t} | x_i \rangle \\ &= \prod_{j=1}^{N-1} \int dx_j \langle x_f | e^{-\frac{i}{\hbar}\hat{H}\epsilon} | x_{N-1} \rangle \langle x_{N-1} | e^{-\frac{i}{\hbar}\hat{H}\epsilon} | x_{N-2} \rangle \dots \langle x_1 | e^{-\frac{i}{\hbar}\hat{H}\epsilon} | x_i \rangle \end{aligned} \quad (1.9)$$

In order to proceed it is appropriate to consider initially only a matrix element $\langle \tilde{x} | e^{-\frac{i}{\hbar}\hat{H}\epsilon} | x \rangle$ which corresponds to one single interval shown in figure (1.1). Using the *completeness relation* again (now for the p -basis) one gets

$$\langle \tilde{x} | e^{-\frac{i}{\hbar}\hat{H}\epsilon} | x \rangle = \int dp \langle \tilde{x} | p \rangle \langle p | e^{-\frac{i}{\hbar}\hat{H}\epsilon} | x \rangle. \quad (1.10)$$

For the case that the Hamiltonian takes the form of equation (1.4) the matrix-element in the integrand depending on p and x can be written as

$$\langle p | e^{-\frac{i}{\hbar}\hat{H}\epsilon} | x \rangle = e^{-i\frac{\epsilon}{\hbar}E} \langle p | x \rangle \Rightarrow \langle p | e^{-i\frac{\epsilon}{\hbar}\left(\frac{\hat{p}^2}{2m} + V(\hat{x})\right)} | x \rangle = e^{-i\frac{\epsilon}{\hbar}\left(\frac{p^2}{2m} + V(x)\right)} \langle p | x \rangle \quad (1.11)$$

which can be proven by using the Taylor-expansion of the exponential function. Remembering that only the one-dimensional case is treated, the inner product $\langle x | p \rangle$ is the wavefunction of the momentum eigenstate p :

$$\langle x | p \rangle = \frac{1}{\sqrt{2\pi\hbar}} \cdot e^{ipx/\hbar}. \quad (1.12)$$

²Here S denotes the classical action

Inserting the last two equations, equation (1.10) becomes

$$\langle \tilde{x} | e^{-\frac{i}{\hbar} \hat{H} \epsilon} | x \rangle \approx \frac{1}{2\pi\hbar} \int dp \left(e^{-i\frac{\epsilon}{\hbar} \left(\frac{p^2}{2m} + V(x) \right)} \cdot e^{-\frac{i}{\hbar} p(\tilde{x}-x)} \right) = \frac{1}{2\pi\hbar} \int dp e^{-i\frac{\epsilon}{\hbar} \left(\frac{p^2}{2m} + V(x) - p\dot{x} \right)} \quad (1.13)$$

with $\dot{x} := \frac{1}{\epsilon}(\tilde{x} - x)$. Introducing a new p -variable defined by

$$p' := p - m\dot{x} \Rightarrow p = p' + m\dot{x}$$

makes it possible to enforce equation (1.13) to become a Gaussian integral³. This leads to an important simplification:

$$\langle \tilde{x} | e^{-\frac{i}{\hbar} \hat{H} \epsilon} | x \rangle \approx \frac{e^{i\frac{\epsilon}{\hbar} \left(\frac{m\dot{x}^2}{2} - V(x) \right)}}{2\pi\hbar} \int dp' e^{-\frac{i\epsilon}{\hbar} \frac{p'^2}{2m}} = \sqrt{\frac{m}{2\pi\hbar i \epsilon}} e^{\frac{i}{\hbar} \epsilon \mathcal{L}(x, \dot{x})}. \quad (1.14)$$

In this equation \mathcal{L} is the one dimensional Lagrangian for a particle with mass m in a potential V :

$$\mathcal{L}(x, \dot{x}) = \frac{m\dot{x}^2}{2} - V(x). \quad (1.15)$$

Furthermore, in the limit $\epsilon \rightarrow \infty$ one can approximate

$$\epsilon \mathcal{L}(x, \dot{x}) \approx \int_0^\epsilon dt \mathcal{L}(x, \dot{x}) = \int_0^\epsilon dt \left(\frac{m\dot{x}^2}{2} - V(x) \right) =: S(\tilde{x}, x), \quad (1.16)$$

where S denotes the action of the classical process where the investigation of the path is started at $t_i = 0$ and ends at $t_f = \epsilon = t/N$. Thus, equation (1.14) becomes

$$\langle \tilde{x} | e^{-\frac{i}{\hbar} \hat{H} \epsilon} | x \rangle \approx \sqrt{\frac{m}{2\pi\hbar i \epsilon}} e^{\frac{i}{\hbar} S(x, \dot{x})}. \quad (1.17)$$

The comparison of this result with the full equation (1.9) leads to the expression for the transition probability (in the last step the discretization of the lattice was assumed):

$$\begin{aligned} K(x_i, 0; x_f, t) &= \langle x_f | e^{-\frac{i}{\hbar} \hat{H} t} | x_i \rangle = \lim_{\epsilon \rightarrow \infty} \prod_{j=1}^{N-1} \int dx_j \left(\sqrt{\frac{m}{2\pi\hbar i \epsilon}} \right)^N e^{\frac{i}{\hbar} S} \\ &= \lim_{\epsilon \rightarrow \infty} \prod_{j=1}^{N-1} \int dx_j \left(\sqrt{\frac{m}{2\pi\hbar i \epsilon}} \right)^N \exp \left(\underbrace{\frac{i}{\hbar} \epsilon \sum_{k=1}^N \frac{m \cdot (x_k - x_{k-1})^2}{2\epsilon^2} - V(x_k)}_{\approx S(x_k, x_{k-1})} \right) \end{aligned} \quad (1.18)$$

Defining the integral over all possible paths from the initial to the final state as

$$\int \mathcal{D}[x] := \lim_{\epsilon \rightarrow \infty} \sqrt{\frac{m}{2\pi\hbar i \epsilon}} \prod_{j=1}^{N-1} \int dx_j \sqrt{\frac{m}{2\pi\hbar i \epsilon}} \quad (1.19)$$

finally produces the tight expression for the path integral

$$K(x_0, 0; x_N, t) = \int \mathcal{D}[x] e^{\frac{i}{\hbar} S} \quad (1.20)$$

which is a measure for the probability of finding a particle at time $t_f = t$ at point $x_f = x_N$ if it was at time $t_i = 0$ at position $x_i = 0$. This integral over all possible paths (equation (1.19)) also can be approximated by a sum over all paths [1].

³In general $\int dx e^{-\alpha x^2} = \sqrt{\frac{\pi}{\alpha}}$ holds

1.2. Numerical evaluation of path integrals

In some cases (e.g. harmonic oscillator) the computational implementation of physical problems requires to perform the sum over 'all paths' of the path integral. An authoritative realization of this is possible by means of the Metropolis algorithm which bases on the Monte Carlo method. The following sections 1.2.1 to 1.2.3 are intended to provide some basics for the illustration of the Metropolis algorithm.

1.2.1. Euclidean path integral and Euclidean action

In the following we will consider the lattice-regulated one-dimensional, quantum mechanical path integral. Introducing imaginary time by $\tau = it$ one can get the so called *Euclidean path integral*, respectively the *Euclidean action* S_E . Since the Feynman path integral (1.20) strongly depends on $\exp(iS/\hbar)$ it is important to study this exponential factor. Considering equation (1.16) yields the exponential factor

$$e^{\frac{i}{\hbar}S} = \exp \left[\frac{i}{\hbar} \int_0^{t/N} dt \left(\frac{m}{2} \left(\frac{dx}{dt} \right)^2 - V(x) \right) \right] = \exp \left[-\frac{1}{\hbar} \underbrace{\int_0^{it/N} d\tau \left(\frac{m}{2} \left(\frac{dx}{d\tau} \right)^2 + V(x) \right)}_{=: S_E} \right] = e^{-\frac{1}{\hbar}S_E}. \quad (1.21)$$

Insertion of $\tilde{\epsilon} := i\epsilon$ into the exponential function of equation (1.18) and its comparison with equation (1.21) leads to

$$e^{-\frac{S_E}{\hbar}} = \exp \left(-\frac{\tilde{\epsilon}}{\hbar} \sum_{k=1}^N \frac{m}{2} \cdot \frac{(x_k - x_{k-1})^2}{\tilde{\epsilon}^2} + V(x_k) \right) \quad (1.22)$$

in which the Euclidean action is given by

$$S_E = \tilde{\epsilon} \sum_{k=1}^N \frac{m}{2} \cdot \frac{(x_k - x_{k-1})^2}{\tilde{\epsilon}^2} + V(x_k). \quad (1.23)$$

Equation (1.22) is an important result, since this equation corresponds directly to the statistical probability weight. This is because equation (1.22) is a damping factor so that it can be understood as the statistical weight for each contribution of the total path integral (see equation (1.20)). Therefore we would like to express expectation values in terms of the Euclidean action. According to statistical mechanics the statistical mean value reads

$$\langle \hat{A} \rangle = \text{Tr}(\hat{\rho} \hat{A}) \quad \text{in which} \quad \text{Tr}(\hat{A}) = \sum_x \langle x | \hat{A} | x \rangle = \sum_x A(x) \quad (1.24)$$

with the density operator only depending on the probability weight $P(x)$ ⁴

$$\hat{\rho} = \frac{P(x)}{\text{Tr}(P(x))}. \quad (1.25)$$

⁴ $P(x)$ is the statistical probability weight for the occurrence of $A(x)$

Assuming that $\mathbf{x}_k = (x_1^{(k)}, \dots, x_N^{(k)})$ is the k th path (or more generally the k th configuration) of the system⁵ results in the expectation value of an arbitrary operator \hat{A} as

$$\langle \hat{A} \rangle = \frac{\text{Tr} \left(\exp \left(-\frac{S_E}{\hbar} \right) \hat{A} \right)}{\text{Tr} \left(\exp \left(-\frac{S_E}{\hbar} \right) \right)} = \frac{\sum_k \langle \mathbf{x}_k | e^{-\frac{S_E}{\hbar}} \hat{A} | \mathbf{x}_k \rangle}{\sum_k \langle \mathbf{x}_k | e^{-\frac{S_E}{\hbar}} | \mathbf{x}_k \rangle} = \frac{\sum_k e^{-\frac{S_E(\mathbf{x}_k)}{\hbar}} A(\mathbf{x}_k)}{\sum_k e^{-\frac{S_E(\mathbf{x}_k)}{\hbar}}} \quad (1.26)$$

where $P(x) = \exp \left(-\frac{S_E(\mathbf{x}_k)}{\hbar} \right)$ has been applied. This result corresponds directly to the mean value of a quantity defined in statistics, in particular

$$\langle \hat{A} \rangle(t) = \text{Tr} \left(\exp \left(-\beta \hat{H} t \right) \hat{A} \right) / \text{Tr} \left(\exp \left(-\beta \hat{H} t \right) \right). \quad (1.27)$$

In the continuous case ($-\infty < x_i < \infty$) equation (1.26) becomes

$$\langle \hat{A} \rangle = \frac{\int \mathcal{D}[\mathbf{x}] e^{-S/\hbar} A(\mathbf{x})}{\int \mathcal{D}[\mathbf{x}] e^{-S/\hbar}} = \frac{\prod_{j=1}^N \int_{-\infty}^{\infty} dx_j e^{-S/\hbar} A(\mathbf{x})}{\prod_{j=1}^N \int_{-\infty}^{\infty} dx_j e^{-S/\hbar}} \quad (1.28)$$

where the factors $\sqrt{\frac{m}{2\pi\hbar\epsilon}}$ of equation have neutralized each other. The Monte Carlo method serves to evaluate the sums or integrals in equations (1.26) or (1.28) numerically [1].

1.2.2. Importance sampling in Monte Carlo Methods

Monte Carlo methods are based on the sampling of N configurations $\mathbf{x}_k \in \Omega$ (Ω denotes the configuration space) whereby the estimate \bar{A} of an expectation value $\langle \hat{A} \rangle$ (e.g. equation (1.26)) can be computed. This is provided by the limit case $N \rightarrow \infty$ in which an estimate \bar{A} equals an expectation value $\langle \hat{A} \rangle$. Uncomfortably a simple random sampling of configuration-points \mathbf{x}_k is inefficient, because points which give a higher contribution to the mean value are not preferred. This is why the Monte Carlo Method proposed by Metropolis is based on the principle of importance sampling. Here the configurations \mathbf{x}_k are not chosen randomly, but more densely distributed in that region of Ω that gives the highest contribution to the mean value. This is effected by introducing a probability-distribution $W(\mathbf{x}_k)$ in equation (1.26) that ensures a higher sampling-rate in the preferred region. According to Metropolis as many iteration-steps as needed to reach the thermodynamic equilibrium⁶ have to be processed initially. Then the probability-distribution corresponds to the Boltzmann-distribution, i.e., the configurations \mathbf{x}_k are sampled with the equilibrium probability $P^{eq}(\mathbf{x}_k) = \exp(-S_E(\mathbf{x}_k)/\hbar)$. Insertion of $P^{eq}(\mathbf{x}_k)$ into equation (1.26) leads to the result that the Monte Carlo estimate simply arises from the arithmetic average of the measurands which are given with constant distances:

$$\langle \hat{A} \rangle = \frac{\sum_{k \in \Omega}^N \frac{\exp(-S_E(\mathbf{x}_k)/\hbar)}{P^{eq}(\mathbf{x}_k)} A(\mathbf{x}_k)}{\sum_{k \in \Omega}^N \frac{\exp(-S_E(\mathbf{x}_k)/\hbar)}{P^{eq}(\mathbf{x}_k)}} = \frac{1}{N} \sum_{k \in \Omega}^N A(\mathbf{x}_k) \quad (1.29)$$

Here N is the total number of states which are generated in all Monte Carlo steps together. Alternatively one can choose the configurations \mathbf{x}_k according to the Boltzmann-distribution with regard to equation (1.28) in order to get the result of equation (1.29) [1]. For the limit case $N \rightarrow \infty$ follows

$$\bar{A} = \frac{1}{N} \sum_{k=1}^N A(\mathbf{x}_k). \quad (1.30)$$

⁵In this assumption one considers each path \mathbf{x}_k to depend on N particle-positions $\{x_i\}$ at corresponding times $\{t_i\}$

⁶Thermodynamic equilibrium: Probability of the single configurations is provided by the Boltzmann-distribution

1.2.3. Markov chains

The numerical implementation of importance sampling described in 1.2.2 can be realized by generating the N configurations \mathbf{x}_k (see equation (1.30)) by means of a Markov process (aka. Markov chain), consisting of several Markov steps [1]. This Markov chain is constructed in such a way, that for $N \rightarrow \infty$ the probability that a configuration \mathbf{x}_k occurs in the Markov chain is given by the equilibrium probability introduced in equation (1.29). In the case of the harmonic oscillator, configurations can be seen as different paths of the concerned particle in a potential V .

In general a Markov chain is described by a $N \times N$ probability-matrix $W(N)$ with $N \leq \infty$. The corresponding matrix-elements $W_{ab} \geq 0$ contain the probability that the concerned system in state x_a fulfills in exactly one Markov step a transition into state x_b . This transition can be written as $x_a \rightarrow x_b$ at which a and b indicate all possible configurations the system can take. Furthermore, in the case of a discrete state system, the condition

$$\sum W_{ab} = 1 \quad \forall a \quad (1.31)$$

is assumed to be satisfied. In the case of a continuous state system, equation (1.31) can be modified so that the matrix W_{ab} changes to a probability density function $W(x_i, x_f) \geq 0$ for a transition $x_i \rightarrow x_f$:

$$\int W(x_i, x_f) dx_f = 1 \quad \forall x_i . \quad (1.32)$$

Until now, the possibility that during the transition $x_i \rightarrow x_f$ several intermediate states x_m with $m = 1, \dots, (n-1)$ are passed through, was not taken into account. Doing this one gets

$$\begin{aligned} W^{(2)}(x_i, x_f) &= \int dx_1 W(x_i, x_1) W(x_1, x_f) \\ W^{(3)}(x_i, x_f) &= \int dx_1 dx_2 W(x_i, x_1) W(x_1, x_2) W(x_2, x_f) \\ &\vdots \\ W^{(n)}(x_i, x_f) &= \int dx_1 \dots dx_{n-1} W(x_i, x_1) W(x_1, x_2) \dots W(x_{n-1}, x_f) \\ &= \int dx_\alpha W^{(n-1)}(x_i, x_\alpha) W(x_\alpha, x_f) . \end{aligned} \quad (1.33)$$

The upper index in brackets denotes the number of steps in the Markov chain which are required for a change from x_i to x_f . For a discrete system of states transition probability matrix of the n th step (cf. equation (1.33)) corresponds to conventional matrix multiplication:

$$W_{ab}^{(n)} = \sum W_{a\alpha}^{(n-1)} W_{\alpha b} , \quad (1.34)$$

with $\sum_b W_{ab} = 1$ and $W_{ab} > 0$ if $P_1, P_b > 0$. In the large n -limit one can proof for the continuous case [1] the relation

$$\lim_{n \rightarrow \infty} W^{(n)}(x_i, x_f) = P^*(x_f) \quad \forall x_i , \quad (1.35)$$

which means that for $n \rightarrow \infty$ the final stationary transition probability density $P^*(x_f)$ resembles the transition probability function. This is an important result, since it says that it is not necessary to know the initial configuration (only the final one) in order to make statements on the probability

function for the transition from the initial to the final configuration. Considering a discrete system of states one finds that $\lim_{n \rightarrow \infty} W_{ab}^{(n)}$ gives a matrix with identical rows that consist of vectors P^* (set of equilibrium probabilities describing the system in $n \rightarrow \infty$).

Taking the large n -limit in equation (1.33) one can proof the previous statement that $P^*(x_i)$ denotes the stationary transition probability density:

$$P^*(x_f) = \int dx_\alpha P^*(x_\alpha) W(x_\alpha, x_f). \quad (1.36)$$

Considering equation (1.32) and $W(x_i, x_f) \geq 0$ one can see that

$$P^*(x_i) \geq 0 \quad \forall x_i \quad \text{and} \quad \int dx_f P^*(x_f) = 1 \quad (1.37)$$

hold. Furthermore it can be shown that P^* is unique ($P(x_f) = P^*(x_f)$).

Summarizing the previous findings, a probability density function $W(x_i, x_f)$ is implemented, which is constructed in such a way that the following three conditions are satisfied:

- $W(x_i, x_f) \geq 0$
- $\int dx_f W(x_i, x_f) = 1$
- $\lim_{n \rightarrow \infty} W^{(n)}(x_i, x_f) = P(x_f)$ (due to uniqueness of P^*)

The probability $P(x_f)$ in the last equation is the equilibrium probability $P^{eq}(x_f)$ introduced in equation (1.29). In other words a valid transition probability density of a Markov chain has been constructed in this procedure, which becomes the stationary transition probability density of the equilibrium in the limit of large Monte-Carlo iterations $n \rightarrow \infty$.

According to [1] a valid choice of $W(x_i, x_f)$ (such that the three conditions are fulfilled) is the detailed balance condition:

$$\frac{W(x_i, x_f)}{W(x_f, x_i)} = \frac{P^{eq}(x_f)}{P^{eq}(x_i)}. \quad (1.38)$$

With the probability $P^{eq}(x_i) = \exp(-S_E(x_i)/\hbar)$ that a configuration x_i occurs in the equilibrium one finds

$$W(x_i, x_f) \propto e^{-S_E(x_f)/\hbar}. \quad (1.39)$$

This means that the transition probability for $x_i \rightarrow x_f$ is proportional to the Boltzmann-factor, only depending on x_f . The bigger an action S_E that corresponds to a state x_f , the smaller is the probability for x_i to perform a transition to x_f in comparison to transitions to all other configurations with smaller action than $S_E(x_f)$. The combination of equation (1.38) and (1.39) yields the ratio

$$\frac{W(x_i, x_f)}{W(x_f, x_i)} = e^{-(S_E(x_f) - S_E(x_i))/\hbar} = e^{-\Delta S_E/\hbar}, \quad (1.40)$$

which is a probability. It indicates, how likely a transition $x_i \rightarrow x_f$ is in comparison to the opposite transition $x_f \rightarrow x_i$. If the condition given by equation (1.40) is satisfied, the generated paths will follow the required Boltzmann-distribution (after a sufficient number of iterations). After reaching the equilibrium, all further generated paths will be equilibrium paths, too [1].

1.2.4. Monte Carlo simulation of paths

For the following considerations it is of importance to note that the numerically chosen configurations \mathbf{x}_k correspond to paths. The discretization of the time-interval into $N - 1$ equally distanced slices leads to N points in time $\{t_k = t_1, \dots, t_N\}$. If the time is discrete, then any configuration (path) \mathbf{x}_k strictly consists of the N corresponding configuration-points $\{x_k = x(t_k) = x_1, \dots, x_N\}$. On the basis of the principles and methods from the previous sections 1.2.1 to 1.2.3, the Monte Carlo algorithm for simulation of path integrals can be constructed in the following way:

1. Initialization
2. Compute action S_E
3. Start Monte-Carlo experiment
 - a) Pick a step x_i
 - b) Propose a shift in the path δx that leads to a new point $x_f = x_i + \delta x$
 - c) Compute $\Delta S_E = S_E(x_f) - S_E(x_i)$
 - d) Proceed Metropolis method to accept/ reject
 - i. if $\Delta S_E \leq 0$: accept since the new configuration-point x_f has lesser action than x_i
 - ii. else: generate randomly a probability $0 \leq P \leq 1$ and accept with $P \leq \exp(-\Delta S_E/\hbar)$ (random experiment was successful)
 - e) if accepted:
 - i. $S_E = S_E + \Delta S_E$
 - ii. $x_i = x_f$
 - f) else: reject (old configuration-point x_i is kept)
 - g) go back to b)

In this regard, one entire run through the discretized lattice with N sites⁷ is called "Monte Carlo sweep". The configuration $\mathbf{x}_k = \{x_1, \dots, x_N\}$ with $k = 1, \dots, M$ thus describes a path after the k th Monte Carlo sweep. If the total number M of Monte Carlo sweeps performed successively is sufficiently large, the paths will fluctuate around the equilibrium state (see comment on equation (1.40)). For the energy E (instead of action S_E) an algorithm can be utilized similarly to that one described above. This implementation will be required to compute several physical quantities.

In summary the algorithm described above is a Markov chain method using importance sampling: In one sweep (iteration) a given point x_i of the path has the probability $W(x_i, x_f)$ to be replaced by another point x_f .

⁷This means to iterate step 3. of the Monte Carlo algorithm N -times, which corresponds to one single round of updating all N lattice points. One single step 3. matches to one point of the path.

1.3. Harmonic and anharmonic oscillator

1.3.1. Implementation of oscillator physics

After having found a respectable way to simulate path integrals in form of the Monte Carlo method, it is aimed to run this algorithm for the case that the particles are located in a potential of an harmonic, respectively anharmonic oscillator. In general the potential of an oscillator reads

$$V(x) = \frac{1}{2}m\omega^2 x^2 + \lambda x^4 = \frac{1}{2}\mu^2 x^2 + \lambda x^4, \quad (1.41)$$

where $\mu^2 > 0$, $\lambda = 0$ provides the harmonic oscillator and μ^2 arbitrary, $\lambda > 0$ the anharmonic oscillator. Examples for oscillator potentials are depicted in figure 1.2. Such physically relevant

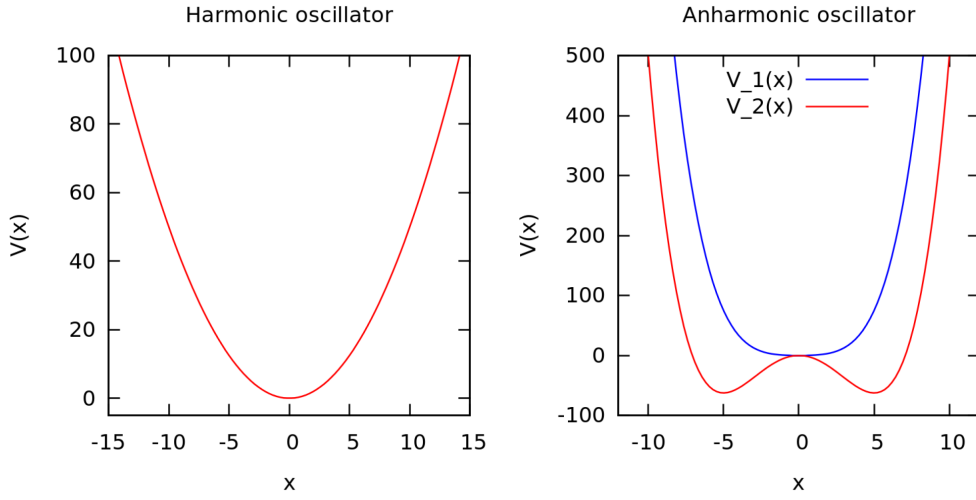


Figure 1.2.: Lefthand: Harmonic oscillator potential with $\mu^2 = 1$. Righthand: Anharmonic oscillator potential $V_1(x)$ with $\mu^2 = 1$, $\lambda = 0.1$ and $V_2(x)$ with $\mu^2 = -10$, $\lambda = 0.1$.

potentials are integrated into the algorithm in terms of the Euclidean action S_E . From equation (1.23) it is known that the discretized Euclidean action is given by

$$S_E = \epsilon \sum_{k=1}^N \frac{m}{2} \cdot \frac{(x_k - x_{k-1})^2}{\epsilon^2} + V(x_k). \quad (1.42)$$

Here a change of notation $\tilde{\epsilon} = i\epsilon \rightarrow \epsilon$ was made in order to simplify the notation. This notation will be kept for the following calculus.

In the computer program the first step consists in choosing a start-configuration \mathbf{x}_1 by random. Then a new configuration is proposed by means of a shift-parameter $\delta x_{i,1}$: From the first element of the initial configuration $x_{i,1} = x_1$ the new path-point $x_{f,1} = x'_1$ is computed by a randomly chosen shift of the initial point (see section 1.2.4). Then the difference of the Euclidean action can be calculated via

$$\begin{aligned} \Delta S_E &= S_E(\mathbf{x}') - S_E(\mathbf{x}_1) \\ &= S_E(x'_1, x_2, \dots, x_{N-1}, x_N) - S_E(x_1, x_2, \dots, x_{N-1}, x_N) \\ &= \epsilon \cdot \left\{ \frac{m}{2\epsilon^2} \left[(x'_1 - x_0)^2 + (x_2 - x'_1)^2 - (x_1 - x_0)^2 + (x_2 - x_1)^2 \right] + V(x'_1) - V(x_1) \right\} \end{aligned} \quad (1.43)$$

Here, only point x_l changed to x'_l . The other points remain unchanged so that most of them eliminate each other. Since periodic boundary conditions are assumed, $x_0 = x_N$ holds. Generalization of equation (1.43) for the l th element of an configuration leads to

$$\Delta S_E = \epsilon \cdot \left\{ \frac{m}{2\epsilon^2} \left[(x'_l - x_{l-1})^2 + (x_{l+1} - x'_l)^2 - (x_l - x_{l-1})^2 + (x_{l+1} - x_l)^2 \right] + V(x'_l) - V(x_l) \right\}. \quad (1.44)$$

1.3.2. Computation of position averages

For the computation of physical quantities such as the groundstate energy E_0 it is necessary to determine position averages first. From equation (1.29) it is known that the arithmetic average of measurands given with constant distances reads

$$\langle \hat{A} \rangle = \frac{1}{N} \sum_{k \in \Omega}^N A(\mathbf{x}_k). \quad (1.45)$$

In this context the position average is generally given with respect to all positions x_l ($l = 1, \dots, N$) of a certain configuration \mathbf{x}_k ($k = 1, \dots, M$) by

$$\langle x_l^n \rangle_m = \frac{1}{m} \sum_{k=1}^m x_l^n(\mathbf{x}_k). \quad (1.46)$$

This is the average of the particle position l to the power of n after $1 \leq m \leq M$ Monte Carlo sweeps. Therefore the average value (y-axis) corresponding to certain Monte Carlo sweep (x-axis) can be generated by

$$\langle x^n \rangle_m = \frac{1}{N} \sum_{l=1}^N \langle x_l^n \rangle_m \quad \text{with an uncertainty of} \quad \Delta \langle x^n \rangle_m = \sqrt{\frac{1}{N} \sum_{l=1}^N (\langle x_l^n \rangle_m - \langle x^n \rangle_m)^2}. \quad (1.47)$$

For the groundstate energy E_0 one initially has to compute $\langle x^2 \rangle$ and $\langle x^4 \rangle$. Furthermore, being able to calculate averages enables the adjustment of the number of Monte Carlo sweeps m that is needed to identify the equilibrium: If one chooses the total number of Monte Carlo sweeps M really large (e.g., $M = 3000$) and plots an observable in dependency of $1 \leq m \leq M$, then one will observe the convergence of this observable to the equilibrium (constant value). The number of sweeps value m_{eq} (here the equilibrium is established) can be read off easily.

1.3.3. Groundstate energy

After an appropriate technique to compute paths numerically was found, it is aimed to determine some physical quantities, e.g., the groundstate energy level E_0 . For that purpose equation (1.27) is considered to get an expression for the time-depending mean Hamiltonian:

$$\langle \hat{H} \rangle(t) = \frac{\text{Tr}(e^{-\beta \hat{H}t} \hat{H})}{\text{Tr}(e^{-\beta \hat{H}t})} = \frac{\sum_{x=0}^n \langle x | e^{-\beta \hat{H}t} \hat{H} | x \rangle}{\sum_{x=0}^n \langle x | e^{-\beta \hat{H}t} | x \rangle} = \frac{E_0 e^{-\beta E_0 t} + \sum_{x=1}^n \langle x | \hat{H} | x \rangle e^{-\beta E_x t}}{e^{-\beta E_0 t} + \sum_{x=1}^n e^{-\beta E_x t}}. \quad (1.48)$$

In this equation the groundstate energy term excluded from the sum has the highest ontribution to the mean value $\langle \hat{H} \rangle(t)$. The reason for this is that for the damping factor $\exp(-\beta E_x t) \leq 1 \forall E_x \geq 0$

(with $x = 0, \dots, n$ and $E_0 < \dots < E_n$) holds. Neglecting the lesser contributing terms it can be approximated

$$\langle \hat{H} \rangle(t) \approx \frac{E_0 e^{-\beta E_0 t}}{e^{-\beta E_0 t}} \quad (1.49)$$

and in the limit $t \rightarrow \infty$ this becomes

$$\lim_{t \rightarrow \infty} \langle \hat{H} \rangle(t) \approx E_0 . \quad (1.50)$$

With the oscillator potential given in equation (1.41) the corresponding Hamiltonian reads

$$\hat{H} = \frac{m}{2} \dot{\hat{x}}^2 + \frac{\mu^2}{2} \hat{x}^2 + \lambda \hat{x}^4 \quad (1.51)$$

Inserting this equation in equation (1.50) then leads to

$$E_0 \approx \lim_{t \rightarrow \infty} \left(\frac{m}{2} \langle \dot{\hat{x}}^2 \rangle + \frac{\mu^2}{2} \langle \hat{x}^2 \rangle + \lambda \langle \hat{x}^4 \rangle \right) \quad (1.52)$$

While $\langle \dot{\hat{x}}^2 \rangle$ and $\langle \hat{x}^4 \rangle$ can be calculated numerically with the technique described in section 1.3.2, this is not possible for the derivative average value $\langle \dot{\hat{x}}^2 \rangle$, which is - according to [1] - given by

$$\langle \dot{\hat{x}}^2 \rangle = \lim_{a \rightarrow 0} \frac{\langle (x_{i+1} - x_i)^2 \rangle}{a^2} = \lim_{a \rightarrow 0} \frac{\langle (x_i - x_{i-1})^2 \rangle}{a^2} . \quad (1.53)$$

This problem can be avoided with the aid of the *Virial theorem*. This theorem provides a relation between the temporal arithmetic mean of the kinetic energy $\langle T \rangle$ and the temporal mean of the potential energy $\langle U \rangle$ of a stable system of N particles. If these N particles do not interact and are influenced by an outer conservative force field provided by a potential $\Phi(\mathbf{r}_k)$ at position \mathbf{r}_k , then the force field is given by $\mathbf{F}_k = -\nabla U = -m_k \nabla \Phi(\mathbf{r}_k)$, where m_k denotes the mass of the k th particle. Using this information the Virial theorem states

$$\langle T \rangle = -\frac{1}{2} \sum_{k=1}^N \langle \mathbf{F}_k \mathbf{r}_k \rangle = \frac{1}{2} \sum_{k=1}^N \langle (m_k \nabla \Phi(\mathbf{r}_k)) \mathbf{r}_k \rangle . \quad (1.54)$$

If the potential in equation (1.54) is considered to be homogeneous of degree n (i.e., $\Phi(\alpha \mathbf{r}_k) = \alpha^n \Phi(\mathbf{r}_k) \forall \alpha > 0$), it is possible to rewrite equation (1.54) using the Euler-equation for homogeneous functions⁸:

$$\langle T \rangle = \frac{n}{2} \sum_{k=1}^N \langle m_k \Phi(\mathbf{r}_k) \rangle = \frac{n}{2} \langle U \rangle . \quad (1.55)$$

With this finding the average total energy E_{tot} can be calculated according to

$$\langle E_{tot} \rangle = \langle T \rangle + \langle U \rangle = \frac{n+2}{2} \langle U \rangle . \quad (1.56)$$

For an oscillator, the potential energy can be splitted up into two summands, that are homogeneous functions of degree $n_1 = 2$, respectively $n_2 = 4$:

$$U = U_1 + U_2 = \frac{\mu^2}{2} x^2 + \lambda x^4 . \quad (1.57)$$

⁸Euler-equation for homogeneous functions $\Phi(\mathbf{r}_k)$ of degree n : $\nabla \Phi(\mathbf{r}_k) \cdot \mathbf{r}_k = n \cdot \Phi(\mathbf{r}_k)$

Taking equation (1.56) into account one gets for the average total energy

$$\langle E_{tot} \rangle = \frac{n_1 + 2}{2} \langle U_1 \rangle + \frac{n_2 + 2}{2} \langle U_2 \rangle = \mu^2 \langle x^2 \rangle + 3\lambda \langle x^4 \rangle . \quad (1.58)$$

In the limit $t \rightarrow \infty$ this becomes the groundstate energy E_0 . In the computer program this will be realized by choosing a sufficiently large number N of time-points (see section 1.2.4).

Furthermore, with the help of equation (1.58), it becomes apparent that only $\langle x^2 \rangle$ and $\langle x^4 \rangle$ have to be determined in order to identify the groundstate energy level. Since the energy E_0 should be computed not before the equilibrium is reached, the value m_{eq} (see section 1.3.2) has to be taken into account. Thus, one gets for position averages

$$\langle x^n \rangle = \frac{1}{M - m_{eq}} \sum_{m=m_{eq}}^M \langle x^n \rangle_m , \text{ with } n = 2, 4 . \quad (1.59)$$

2. Implementation

The Monte Carlo simulation is carried out on a 1-Dimensional discrete time lattice with a lattice spacing a which is just the imaginary time sliced into smaller intervals. A path is generated by either random sampling which amounts to a hot start or all the values of the path are 0.0 which is called a cold start. With the path generated, the burn-in phase is passed with a thermalization run of several Monte Carlo iterations. Once equilibrium is reached, a meaningful extraction of observables and properties can be made all of which are outlined below.

2.1. The Harmonic Oscillator

2.1.1. Mean Square Position

The first meaningful observable that was measured and worked on here was the mean square position. Monitoring the change in this observable with the iterations of the Monte Carlo simulation, showed its increase to a certain value after which the observable merely showed statistical fluctuations around this mean value. This value can be compared to the one obtained from an analytical expression in discrete lattice theory,

$$\langle x^2 \rangle = \frac{1}{2\mu(1 + a^2\mu^2/4)^{1/2}} \left(\frac{1 + R^N}{1 - R^N} \right) \quad (2.1)$$

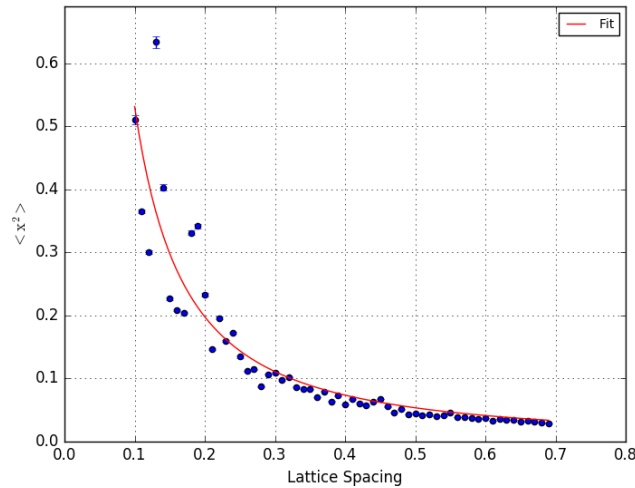


Figure 2.1.: The mean squared position value was consistently around 0.5, it's true value, over several iterations and decreased with an increase in the lattice spacing.

where $R = 1 + a^2\mu^2 - a\mu(1 + a^2\mu^2/4)^{1/2}$. The measured value was consistently (0.51 ± 0.004) for a particular lattice spacing which here for a discrete lattice is a time step of 0.1 units and a $\mu^2 = 1$. This is in very nice agreement with the one calculated from equation (2.1). The mean value of mean squared positions changes with lattice spacing as shown in figure 2.1 with 0.5 being the true value in the continuum limit. The fluctuations can be seen in the plot alongside a plot of the ground state probability density of a harmonic oscillator as obtained from the Monte Carlo Simulation in figure 2.2.

2.1.2. Energy Levels

The ground state energy level was measured aided by the Virial theorem from which we have that for the harmonic oscillator,

$$E_o = \mu^2 \langle x^2 \rangle \quad (2.2)$$

With (0.51 ± 0.004) being the measured mean square position value, the same was obtained as the value of the energy when $\mu^2 = 1$. This is again, in reasonable agreement with the theory.

2.1.3. Ground State Probability Density

Following the method outlined in Creutz and Freedman [1], the x axis was divided in to bins and the number of lattice points which fall into each bin were counted for an ensemble of paths. Normalizing this by the total number of points counted, gives the ground state probability density as shown in figure 2.2. The plot shown here is really the result of the use of the Gaussian Kernel Density Estimation algorithm but is in essence the same method but with a smooth curve fit (the probability density function) to the distribution and was done after the first method was put in to use and had proved successful.

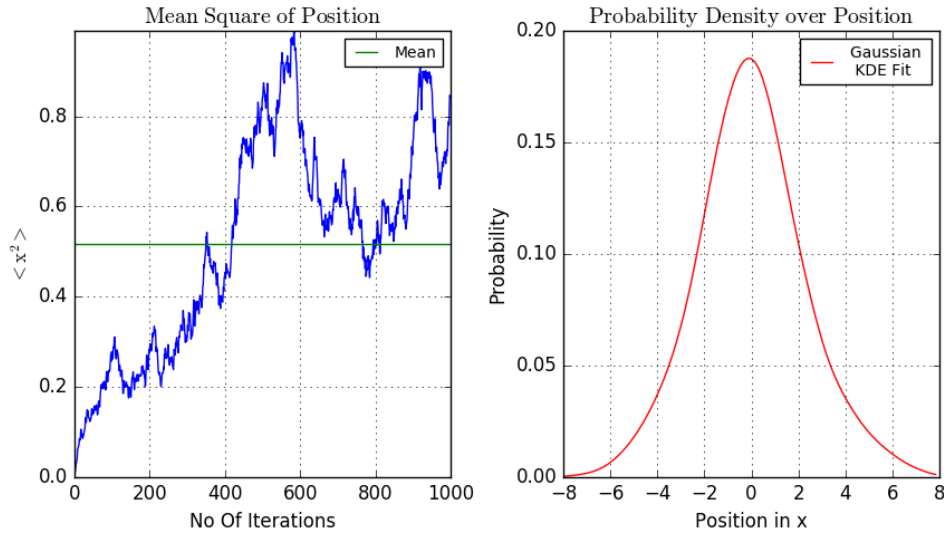


Figure 2.2.: For a lattice spacing of around 0.1, the mean squared position value was here, (0.5132 ± 0.004) . Next to it, is a Gaussian (or nearly) ground state probability density for the Harmonic Oscillator.

2.1.4. Autocorrelation of Monte Carlo estimates of observables

The formula for σ or the standard deviation assumes that the N measurements are all independent. Since successive values of paths are generated from each other, this is never true in a Monte Carlo simulation. The position values are more and more related the less time one waits between measurements. It is therefore important to be able to estimate how many iterations are required between paths in order for them to become uncorrelated. A form of the autocorrelation function can be defined as,

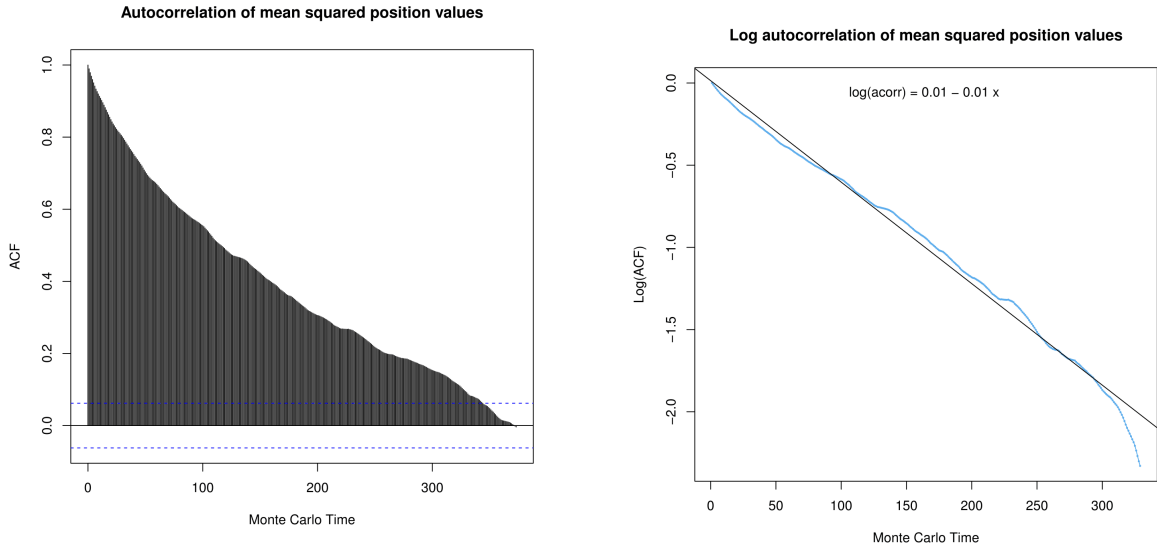
$$\Gamma(t) = \frac{\langle (y(0) - \bar{y})(y(t) - \bar{y}) \rangle}{\langle (y(0) - \bar{y})^2 \rangle} \quad (2.3)$$

where t is the Monte Carlo Time or in plainer words, the number of iterations, y is some observable (like the mean square position) and \bar{y} is the mean of the measured values of y . The autocorrelation function should decay exponentially with t :

$$\Gamma(t) = \exp(-t/\tau) \quad (2.4)$$

where τ is the autocorrelation time. It gives a measure of the number of iterations needed between measurements for them to be reasonably uncorrelated.

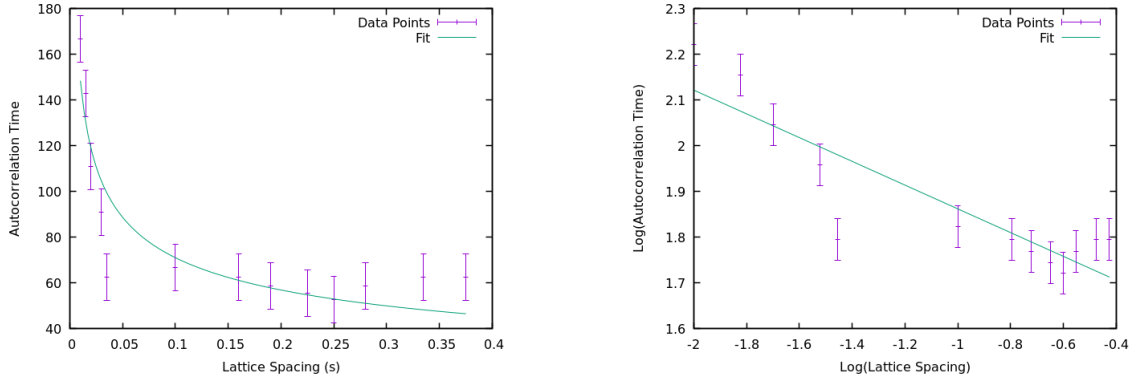
The in-built `acf()` function in R was used to calculate the same autocorrelation function and is as shown in figure 2.3a for a lattice spacing of 0.1. The exponential decay of the autocorrelation is more evident when the log plot is made as is done in figure 2.3b. This is observed only at low Monte Carlo time with large statistical fluctuations beyond 150 iterations taking over, the linear fit is no longer feasible. But in the range where it is possible, the autocorrelation time can be measured from this linear fit, it just being the $-1/\text{slope}$.



(a) Autocorrelation Function of Mean Square Position for the Harmonic Oscillator (b) Linear fit for log of the autocorrelation function

Figure 2.3.: Autocorrelation Function for the Harmonic Oscillator

Once this was definitive, the autocorrelation time was measured as a function of the lattice spacing for the mean square position shown here in figure 2.4a. It seems to follow some sort of



(a) Autocorrelation Time of Mean Square Position for the Harmonic Oscillator as a function of the lattice spacing
(b) The linear fit suggests a power law relation between the Autocorrelation Time and the lattice spacing

Figure 2.4.: Autocorrelation Times against Lattice Spacing

power law which again can be established through a log-log plot as shown alongside it in figure 2.4b.

Applying the fit which predictably was linear and obtaining the parameters, we get a relation between the autocorrelation time and the lattice spacing in the range for -

$$\tau = 4.96a^{-0.25} \quad (2.5)$$

This is a relation that holds for the mean square position as measured here, it could be different for a different observable (*A confession has to be made here - There seems to be a large error in the calculation of the parameters or in the actual autocorrelation itself that perhaps stems from some incorrect assumption made or incorrect or insufficient data points. The fit parameters and the resulting expression overestimates the autocorrelation time. We have been unable to zero in on a solution here.*).

2.1.5. Optimizing Δ

In the Metropolis Algorithm, the new position values were chosen arbitrarily from a range: $x_j - \Delta < x'_j < x_j + \Delta$. The choice of this parameter is constrained by the acceptance probability in the Metropolis algorithm as is clear by the fact that a large deflection, as we shall refer to this Δ from here, the change in action will be very large and hence the probability of acceptance will be small. It also affects the autocorrelation times. For small deflections, it will take many iterations for the value of a given lattice to change significantly, giving a large autocorrelation time. Conversely for large deflections the probability of acceptance is low, leading also to a large autocorrelation time. It is therefore expected that there is some optimal value of the deflection for which the autocorrelation time is at a minimum while at the same time the acceptance probability is reasonably high.

In figure 2.5, we see how the acceptance probability changes with the deflection. A general criterion for choosing this deflection as given by Creutz and Freedman [1] is $\Delta = 2\sqrt{a}$ which for $a = 0.1$ is 0.63 giving an acceptance probability of 0.5. The same was used and with inspection it was found to be optimal around 0.7, giving an acceptance probability in excess of 0.5. This is perhaps

a result of the effect of the autocorrelation time, being minimum around the same deflection value here.

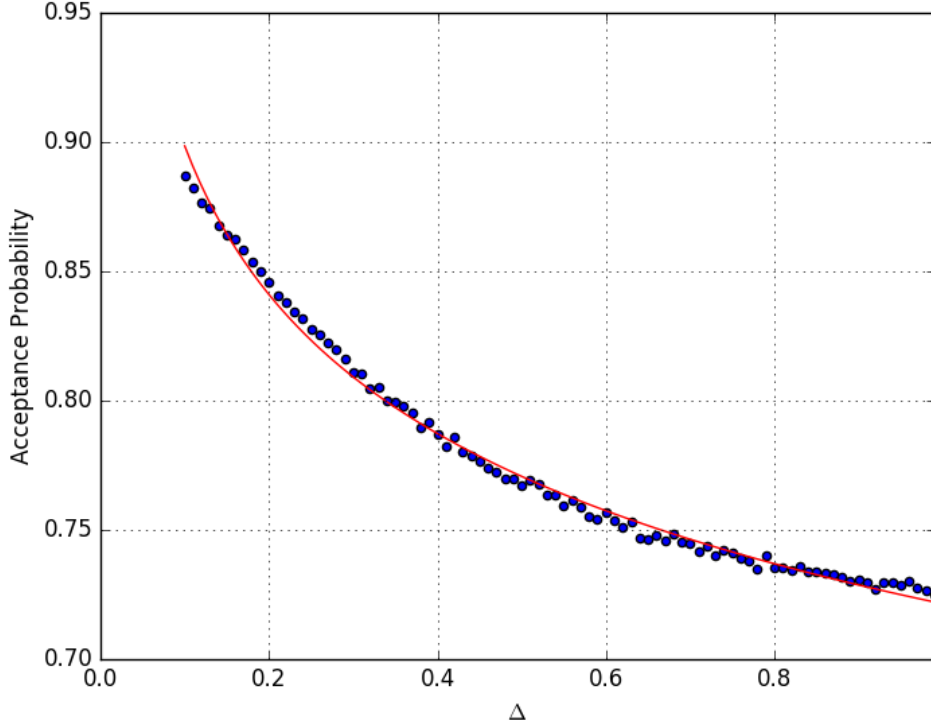


Figure 2.5.: Acceptance Probability against Deflection

2.2. The Anharmonic Oscillator

2.2.1. Mean Square Position, Ground State Probability Density and Autocorrelation

By just modifying the potential:

$$V(x) = \lambda(x^2 - f^2)^2 \quad (2.6)$$

The harmonicity is lost. The quartic term brings the anharmonic case which was dealt with in the same manner as the harmonic case with $\lambda = 1.0$. Again, by inspection, an appropriate f was selected noting how the results diverged for higher f . Obtained in the same manner as the harmonic oscillator, the probability density here has a bimodal distribution or one much like a sum of gaussians, with the minimums occurring at around the value of f . The mean square position usually fluctuated around (1.2 ± 0.01) . The energy of the Anharmonic Oscillator is not as straightforward as in the Harmonic case because of the quartic term which adds to it.

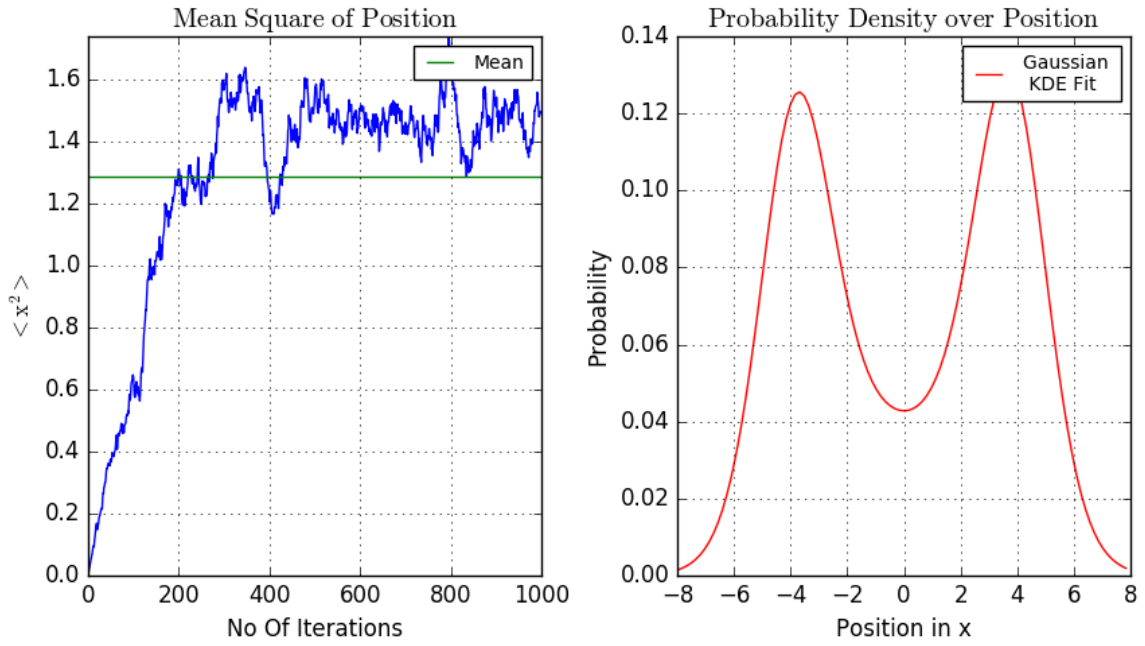
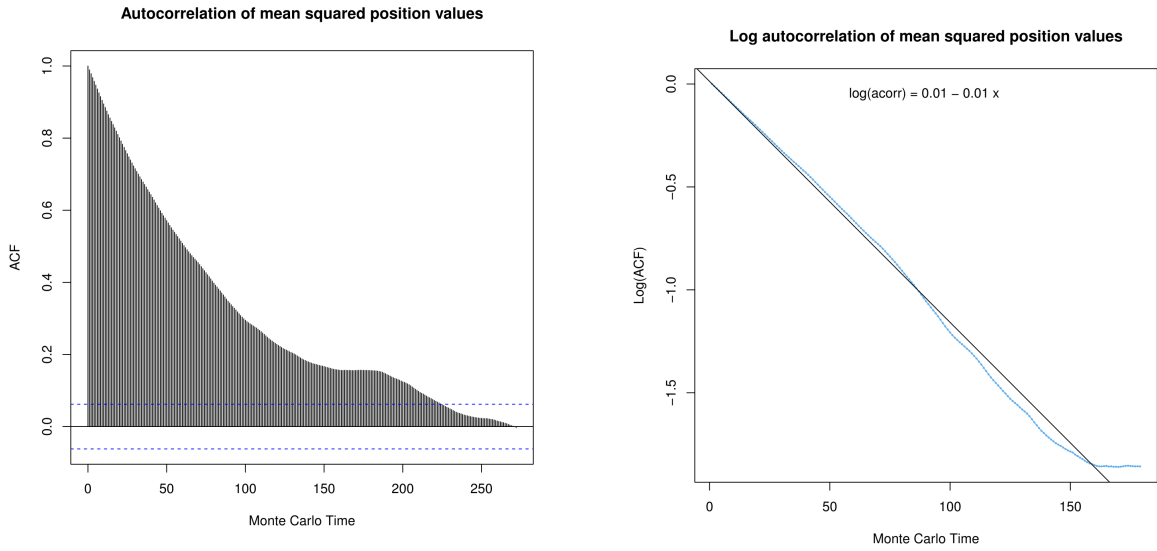


Figure 2.6.: For a lattice spacing of around 0.1, the mean squared position value was here, (1.3 ± 0.01). Next to it, is the ground state probability density for the Anharmonic Oscillator.



(a) Autocorrelation Function of Mean Square Position for the Anharmonic Oscillator

(b) Linear fit for log of the autocorrelation function

Figure 2.7.: Autocorrelation Function for the Anharmonic Oscillator

3. Conclusion

Here we studied the Quantum Harmonic Oscillators in the path integral formulation using the Metropolis algorithm, a Markov Chain Monte Carlo method to generate paths to calculate one observable, the lowest energy level and the ground state probability density. The lowest energy value and the mean squared position observable had a value of around 0.5. In addition, for the harmonic oscillator we made measurements of the autocorrelation time and other parameters to run effective code. For the energy levels of the harmonic oscillator the lattice spacing and β parameter seem to influence the agreement with theoretical values.

All calculations were made for finite discrete lattice spacing. More accurate continuum values are obtainable only with smaller lattice spacing but this naturally significantly increases computation time, not to mention the rapid increase in autocorrelation. This problem was developed with one dimensional discretization, so with more dimensions, space-time discretization and the like, again, more computational power is required.

The use of this method for the Harmonic Oscillator is redundant and unnecessary since it is one of two problems for which an analytical solution exists with a closed form expression of the path integral. The method is particularly useful for more complicated systems like the anharmonic oscillator. Still, the method helps verify and reinforce the understanding of the harmonic oscillator and this project was quite instructive in helping understand the methods involved considering how indispensable it is in the fields of QCD, Network Analysis, Molecular Dynamics.

Acknowledgements

We would like to thank Dr. Serdar Elhatisari for tutoring us on the topic and helping fix bugs in our code. We would of course want to thank Dr. Professor. Urbach for the opportunity as part of his illuminating course on Computational Physics during WT2016.

List of Figures

1.1. Division of the interval	4
1.2. Potentials of harmonic and anharmonic oscillator	11
2.1. The mean squared position value was consistently around 0.5, it's true value, over several iterations and decreased with an increase in the lattice spacing.	15
2.2. For a lattice spacing of around 0.1, the mean squared position value was here, (0.5132 ± 0.004) . Next to it, is a Gaussian (or nearly) ground state probability density for the Harmonic Oscillator.	16
2.3. Autocorrelation Function for the Harmonic Oscillator	17
2.4. Autocorrelation Times against Lattice Spacing	18
2.5. Acceptance Probability against Deflection	19
2.6. For a lattice spacing of around 0.1, the mean squared position value was here, (1.3 ± 0.01) . Next to it, is the ground state probability density for the Anharmonic Oscillator.	20
2.7. Autocorrelation Function for the Anharmonic Oscillator	20

Bibliography

- [1] M. Creutz and B. Freedman, *A Statistical Approach to Quantum Mechanics*, Annals of Physics **132**, 427-462 (1981).
- [2] R.P. Feynman and A.R. Hibbs, *Quantum Mechanics and Path Integrals*, McGraw-Hill, New York, 1965
- [3] Colin Morningstar, *The Monte Carlo method in quantum field theory* arXiv:hep-lat/0702020 (2007)
- [4] Joseph Marie Thijssen, *Computational Physics*, Cambridge University Press, 2007, Print.

A. Bootstrap error analysis

The error analysis was done with the bootstrap method. A set of B bootstrap samples are taken by random sampling with replacement such that each bootstrap sample contains N data points. For each of the samples the mean value is computed and there are B bootstrap means $\{\bar{X}_i\}$. The mean and standard deviation of these give the bootstrap estimate of the mean of the underlying distribution and its standard error.